Trans Indian Inst Met (2017) 70(10):2707–2717
DOI 10.1007/s12666-017-1131-9

TECHNICAL PAPER

Effect of Flyash Treatment on the Properties of Al-6061 Alloy Reinforced with SiC–Al_2O_3–C Mixture

R. Govinda Rao[1] · K. L. Sahoo[2] · R. I. Ganguly[1] · R. R. Dash[1] · N. Narasaiah[3]

Received: 17 January 2017 / Accepted: 6 April 2017 / Published online: 27 April 2017

Abstract Studies are conducted on an Al-6061 alloy reinforced with in situ ceramic mixture (Al_2O_3–SiC–C). The mixture is prepared by carbothermal reduction of fly-ash in a plasma reactor, where SiO_2 is converted to SiC. The strength values for Al-6061-flyash (FA) and Al-6061-plasma synthesized flyash (PSFA) composites are 35% and 63% higher than that of the Al-6061 alloy. Wear resistance of the developed alloy composite prepared with treated flyash (Al-6061-PSFA) has increased two-fold in comparison to virgin alloy (Al-6061) and 1.5 fold higher in comparison to a similar alloy composites prepared with untreated flyash (Al-6061-FA). The unique property of the developed alloy composite is due to harder SiC particle reinforcement. Excess carbon in the form of graphite and the unique morphological feature of microstructure have enhanced the properties such as strength and wear resistance of the developed alloy composite.

Keywords Aluminium alloy · In-situ ceramic composite · Flyash · Wear · Plasma rector

✉ K. L. Sahoo
klsahoo@gmail.com

[1] Metallurgical Engineering Department, Gandhi Institute of Engineering and Technology, Gunupur, Odisha 765022, India

[2] CSIR-National Metallurgical Laboratory, Jamshedpur, Jharkhand 831007, India

[3] National Institute of Technology, Warangal, Telangana 506004, India

1 Introduction

Use of Al-based metal matrix composites (MMCs) as structural materials is advocated by several researchers [1–4]. Among different discontinuous reinforcements used, flyash (FA) is considered to be a potential candidate for production of Al-based MMCs. Basically flyash is an inexpensive reinforcing agent consisting of particles such as SiO_2, Al_2O_3, as major constituents. Components such as piston, engine cover, and connecting rods are made of Al-particle reinforced composites [5, 6]. By addition of flyash to Al matrix, hardness reaches a value ranging between 65 and 82 HB. The scope for cast Al-based flyash composite has further increased due to improved wear resistance [6]. This has led to the acceptability of the Al-based flyash composite for yet wider applications in automotive small engine parts as well as in electric machines. Rohatgi et al. [4] successfully produced automobile components with Al-356 alloy flyash composite adopting stir casting method. They reported uniformity in the microstructure in terms of particle distribution in the alloy matrix for small castings. Thus, scope for research in alloys with flyash addition has increased [5–8].

Al-based flyash composites are prepared by different routes such as powder metallurgy technique [9, 10] and stir casting technique [11, 12]. Extensive work on wear behaviour of Al-based composites, prepared by using SiC/Al_2O_3/graphite or flyash individually or in combination as reinforcement in the matrix, has been reported [5]. Milan and Bowen [13] have shown the effects of particle size, particle volume fraction, and matrix strength on the properties of SiC reinforced Al-alloys. The morphology and distribution of reinforcement have large effect on strength as well as abrasion resistance. It is well established that the abrasion resistance increases with increase in volume fraction of the reinforcement [4, 14]. However, there exist

Table 1 Chemical composition of flyash in as received condition and after magnetic separation

Elements	Composition (wt%)						
	SiO_2	Al_2O_3	CaO	TiO_2	Fe_2O_3	C	MgO
As received flyash	62	27	2	1	5	0.35	0.5
After magnetic separation	64	28	2.5	1.5	0.5	0.5	1

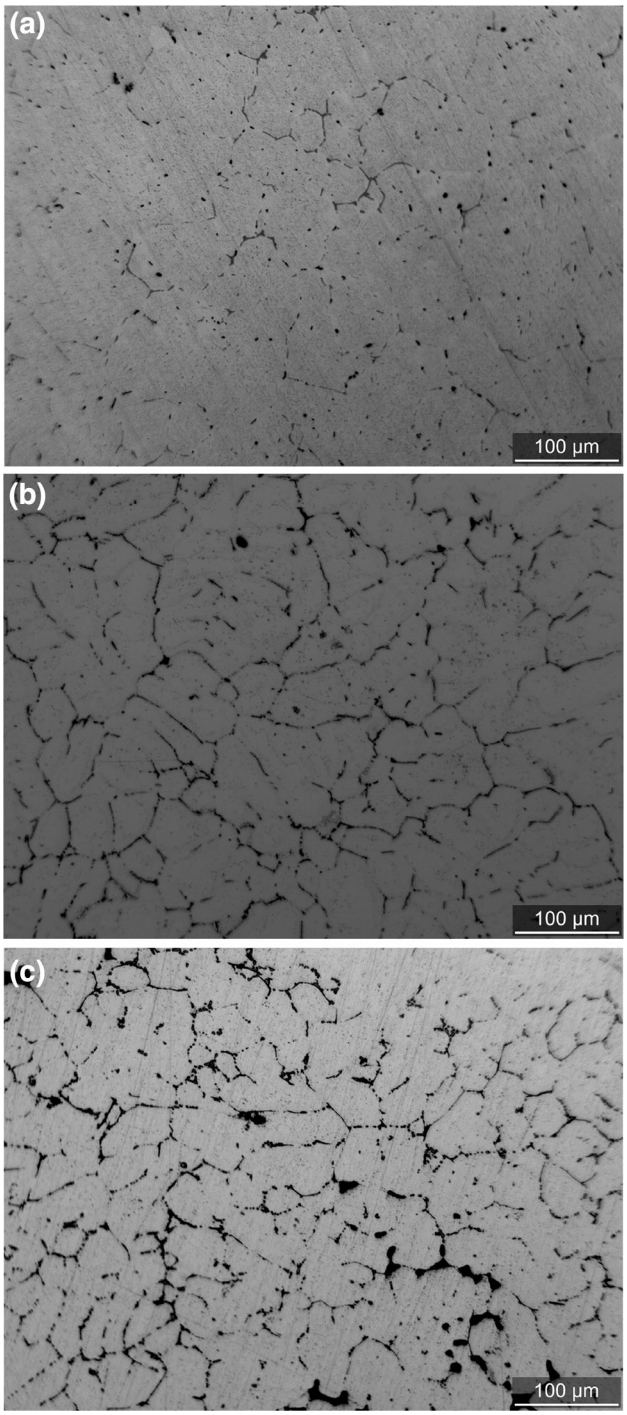

Fig. 1 Microstructures of **a** Al-6061 alloy, **b** Al-6061-FA composite, and **c** Al-6061-PSFA composite

controversial reports [14, 15] on the effect of volume fraction and aspect ratio of the reinforcement on wear behaviour of Al-alloy based composites. Sahin et al. [15] have prepared Al-SiC (up to 55 vol%) composite by vacuum infiltration technique. The composite shows increased wear resistance until the volume fraction reaches 10%. Graphite in hybrid Al-based composites reduces the coefficient of friction and thereby, improves machinability and wear resistance [16]. However, the addition of higher volume fraction of graphite increases the porosity and thereby, decreases tribological and mechanical properties [17]. Literature has also reported that Al alloy-SiC composite shows enhancement of tensile strength up to 10 vol% of reinforcement and then the strength decreases with higher volume fraction of SiC addition [18].

Flyash addition is an alternative mean to dispense with costly powder such as SiC and/or Al_2O_3. Literatures have reported wear resistance of Al-based flyash composite similar to that of Al–Al_2O_3 and/or Al–SiC composites [4, 19]. With changes in working parameters such as load, sliding distance, speed and other experimental conditions during test, mechanism of wear also changes [14]. The matrix such as Al and/or its alloys get work hardened to different extent depending on load as well as length of time of exposure. The matrix may also get heated causing microstructural changes. There is also interplay between debris on the surface of work piece and the matrix. Therefore, studies on the wear behaviour of Al-flyash composite is thought to be an interesting proposition.

The authors' group have developed a unique ternary ceramic mixture by carbothermal treatment of colliery shale material which contains SiO_2–Al_2O_3–C [20, 21]. Colliery shale is similar in composition to that of flyash. Since flyash is abundantly available in power plant, therefore similar experiments have been carried out in the present investigation to convert SiO_2 to SiC. Microstructural studies have revealed morphological changes in the treated flyash which will improve strength and toughness of Al-based flyash composite material. This paper has emphasized more on studies on the wear behaviour of novel Al-6061 alloy based composites. Al-based plasma synthesized flyash (PSFA) composite has been prepared with newly developed ternary ceramic mixture. For comparison purpose, Al-6061-FA composite of similar volume fraction has been used.

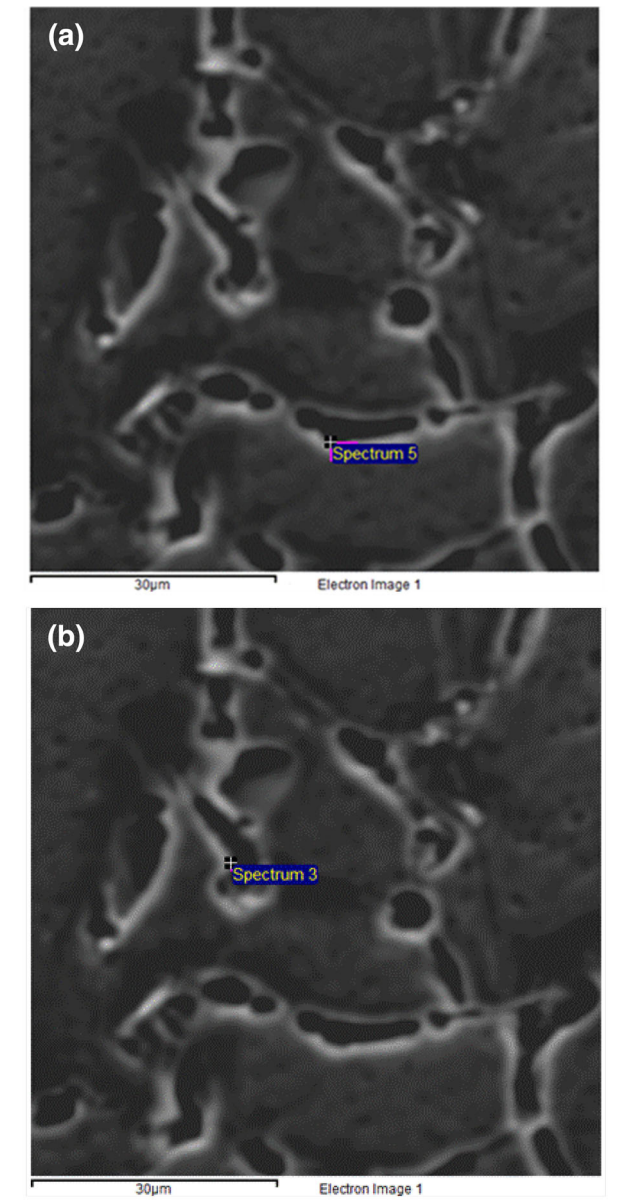

Fig. 2 **a**, **b** SEM micrograph with EDS analysis at the grain boundary of Al-6061-FA composite **b**, **c** SEM micrograph with EDS analysis at the grain boundary of Al-6061-PSFA composite

2 Experimental

2.1 Flyash Synthesis

Flyash was sieved and below 40 µm powders were used for experimentation. A dressing treatment was given to flyash by wet magnetic separator for removal of Fe_2O_3 present in it. The flyash was then dried and mixed with requisite amount of activated charcoal. Powders were thermally treated in plasma reactor. Both as received as well as thermally treated flyash powder were characterized with SEM, XRD, and EDS.

2.2 Preparation of Al-6061 Alloy Based Composites

Al-6061 alloy was melted in a bottom pouring furnace, fitted with a stirrer. Argon gas was passed throughout the melting operation to avoid oxidation. Flyash particles were pre-heated to 600 °C in a muffle furnace for enhancing wettability of powder with liquid melt. Preheated particles were poured into the vortex, created by rotating stirrer at a speed of 400 rpm. The Al-alloy based composites were prepared with treated as well as untreated flyash. Composites prepared with untreated flyash was used for comparison purpose. The molten Al-6061alloy composite was poured into a preheated (150 °C) rectangular metallic mould.

2.3 Microstructural Characterization of Composites

Microstructures of the cast alloy based composite specimens were examined by both optical microscope and SEM.

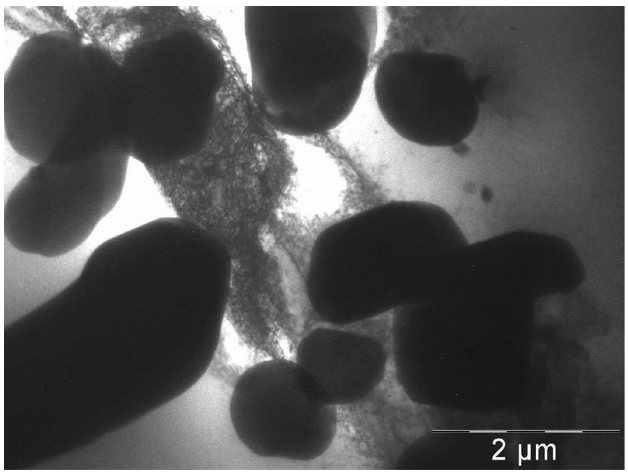

Fig. 3 Representative TEM micrograph of Al-6061 alloy based composite indicating uniformity of flyash particles dispersed in the matrix

Table 2 Physical and mechanical properties of base alloy and composites

Material	% of volume fraction of flyash	Density (g/cc)	Hardness (HV)	UTS (MPa)	% of strength improved compared to Al-6061alloy (%)	% Elongation	Fracture strain
Al-6061alloy	0	2.70	45	139	–	26	0.34
Al-6061-FA composite	10	2.54	60	187	35	15	0.33
Al-6061-PSFA composite	10	2.58	77	227	63	16	0.30

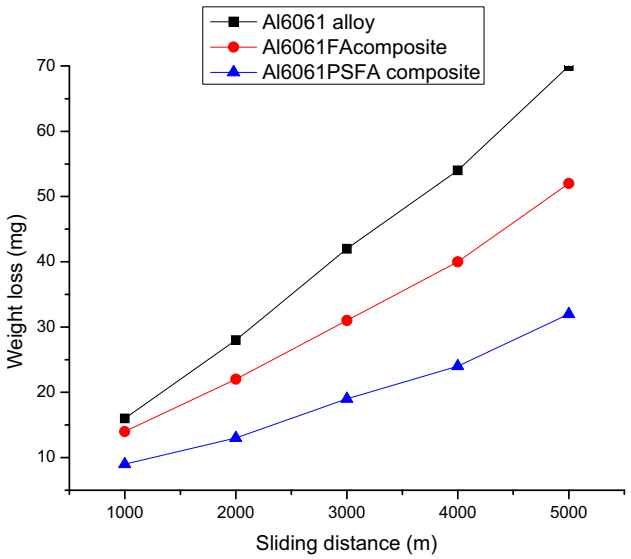

Fig. 4 Variation of weight loss with sliding distance (Load: 60 N, Speed: 1.16 m/s)

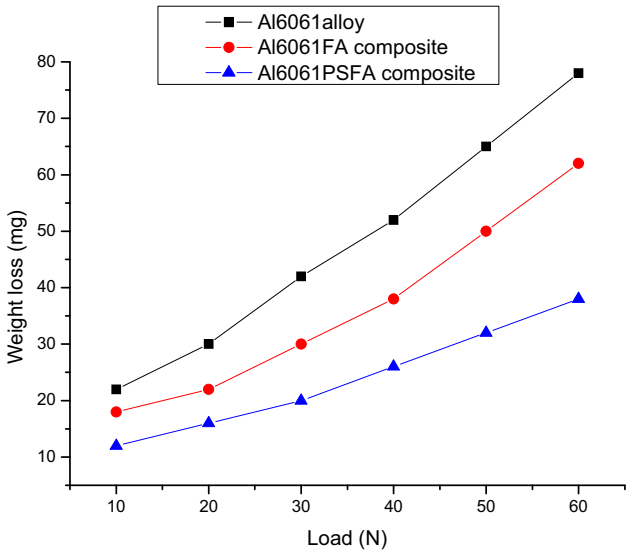

Fig. 5 Variation of weight loss with load (Speed: 1.16 m/s, sliding distance: 5000 m)

Energy dispersive X-ray analysis was carried out at 20 keV, and the results reported were the average of 5 readings for each phase. The volume fraction and size distribution of the precipitates and particles were estimated with the help of an image analyzer (XJL-17). X-ray diffraction analysis was carried out with a diffractometer equipped with Cu target. Hardness was measured in a digital Vicker's hardness tester under a load of 5 kg and the average of ten readings was reported. Tensile specimens were prepared according to the ASTM E8 M standard. These specimens were tested by an Instron machine at room temperature at a strain rate of 2×10^{-4} s^{-1}.

2.4 Dry Sliding Wear Test

Dry sliding wear tests were carried out on pin-on-disc type wear testing machine (DUCOM TR201LE). The geometry of test samples used for wear test was 8 mm in diameter and 40 mm in length. Samples were placed on a rotating disc (EN31 steel disc of hardness 65 HRC). The geometry of contact surfaces of pin and disc were flat on a flat surface. The surfaces were polished to a roughness of $R_a = 0.1$ μm before each wear test. Wear tests were conducted at three test conditions i.e. (1) varying loads from 10 to 60 N (at constant speed 2.03 m/s, sliding distance 5000 m), (2) varying sliding distance from 1000 to 5000 m (at a constant load 60 N, speed 2.03 m/s), (3) varying speed between 1.03 and 2.66 m/s (at a constant load of 40 N, sliding distance 5000 m). The wear was measured in terms of decrement in length, recorded by LVDT fitted in the instrument. LVDT record did not uniformly showed the length change due to lack of uniform surface contact. Therefore, weight loss was taken as a measure of wear in the present investigation. Weight loss was determined by digital weighing balance with an accuracy of ±0.01 mg. Each test was conducted three times and average weight loss was taken as a measure of wear. Worn out surfaces were examined by SEM–EDS analysis.

3 Results and Discussion

3.1 Flyash Characterization

The chemical composition of flyash is shown in Table 1. It contains SiO_2, Al_2O_3, and Fe_2O_3 as major constituents. Fe_2O_3 in flyash is an undesirable compound since it combines with Al and forms Al–Fe–O compounds and or needle shaped Al-silicides, which reduces the fracture strength of the MMCs. Therefore, flyash is treated in a wet magnetic separator. By treatment, quantity of Fe_2O_3 is brought down from 5 to 0.5% (Table 1). The average size of the powder particle is around 15 µm. This is done because the properties of the composite depend on the size, shape, distribution, and volume fraction of reinforcement particles. In the treated flyash, SiO_2 is fully converted to SiC in the presence of excess carbon over the stoichiometry requirements.

3.2 Microstructural Characterization

Al-6061 alloy contains (wt%) Cu: 0.30, Mg: 0.81, Si: 0.68, Mn: 0.31, Fe: 0.24, and rest Al. Other elements such as Ti, Cr, and Zr are present in minor quantity. Figure 1a–c show optical micrographs of Al-6061 alloy, Al-6061-FA composite and Al-6061-PSFA composites, respectively. In both Al-6061-FA and Al-6061-PSFA composites, thickening of grain boundaries are observed due to segregation of reinforcement materials. In addition, flyash particles are scattered within the grains, i.e., within the matrix. No distinct non-uniformity of dispersion of composite particles within the grain body is found. Samples for micrographs are chosen randomly from the cast products. Presence of elements such as Al, Si, Ti, and O in Al-6061-FA composite (Fig. 2a) and Al, C, Si, O, Cu, Cr etc. in Al-6061-PSFA composite (Fig. 2b, c) are observed. The elemental analysis (Fig. 2c) by EDS confirms presence of flyash particles at the grain boundaries. A representative transmission electron

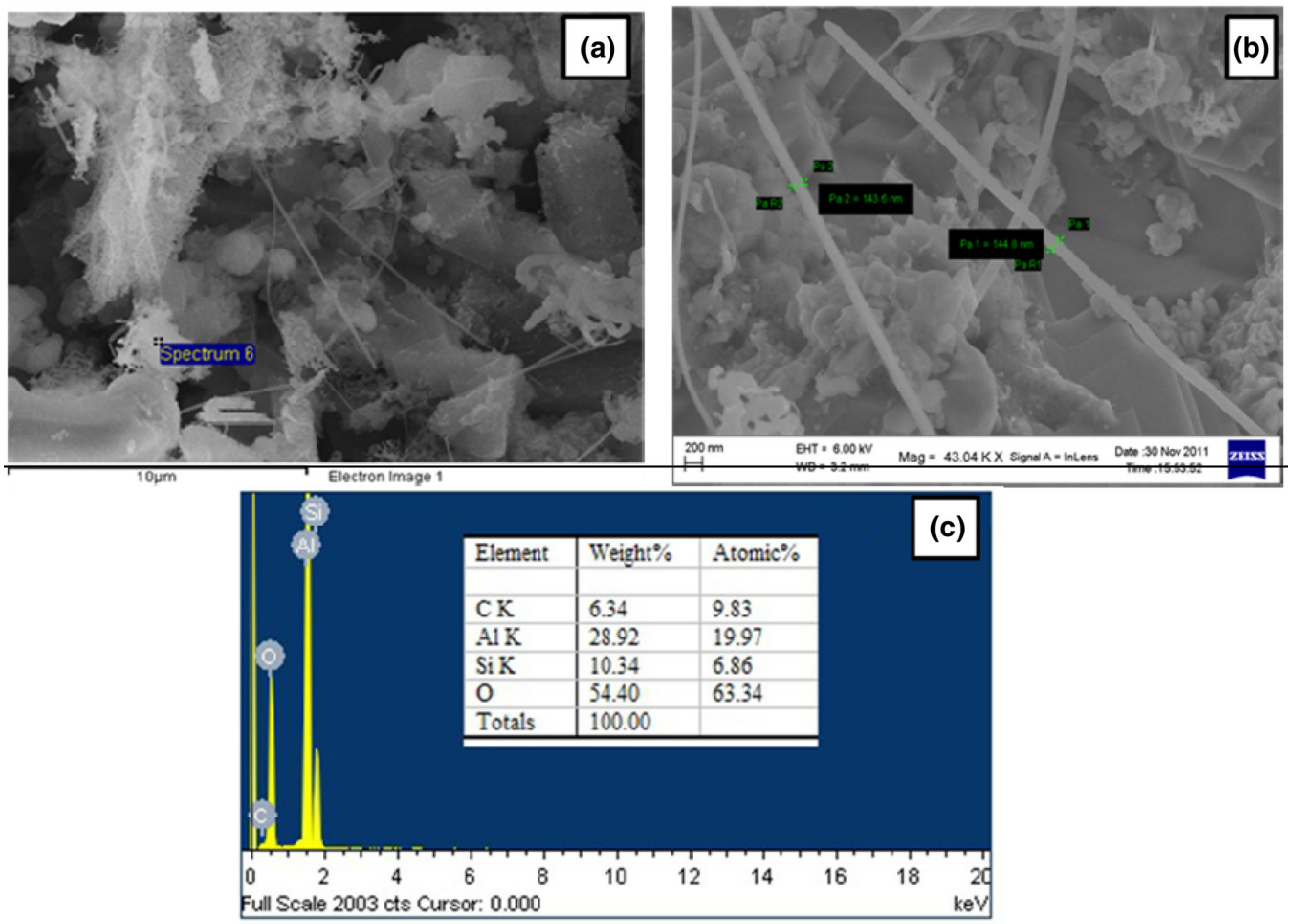

Fig. 6 **a**, **b** SEM micrographs **c** EDS analysis of plasma treated flyash

microscopy (TEM) image of Al-6061 alloy based composite is shown Fig. 3 to indicate uniformity of flyash particles dispersed in the matrix.

3.3 Physical and Mechanical Properties of Composite

Table 2 shows physical and mechanical properties of all the three materials. The density of composites is lower than that of virgin alloy. This will increase specific strength of the material. Both hardness and tensile strength of Al-6061-PSFA composite are found to be the highest among the three materials. The strength values for Al-6061-FA and Al-6061-PSFA composites are 35 and 63% higher than that of the virgin alloy. Similar trends are observed for hardness values as well. However, the elongation values for the composites are substantially lower. True fracture strain, that is the maximum true strain that a material can withstand before fracture, is calculated for all three materials and is included in Table 2. There is no significant difference in true fracture strain value of the Al06061 alloy and the fly ash composite material.

3.4 Tribological Properties

Figure 4 shows wear behaviour of the three materials, namely Al-6061 alloy, Al-6061-FA and Al-6061-PSFA composites. Three curves are superimposed for drawing comparison in performance of those materials put under identical conditions during wear run. For all the sliding distance, the developed Al-6061-PSFA alloy composite has shown the highest abrasion resistance among the three materials. The magnitude of weight loss at all the sliding distance for Al-6061-PSFA composite is 1.5 times lesser if compared with the alloy composites prepared with untreated flyash. The virgin alloy has shown the least resistance i.e. loss in weight is twofold higher if compared with Al-6061-PSFA composite and 1.5 fold higher if compared with the Al-6061-FA composite. Similar trend is observed from the plot of test results shown in Fig. 5. The curves narrate the effect of test load on the weight loss of the three materials, tested under identical conditions (i.e.: speed 1.16 m/s, sliding distance 5000 m).

Improved tribological properties of the novel composite are resulted by the addition of developed ternary ceramic mixture into the Al alloy matrix. Flyash essentially contains Al_2O_3, SiO_2 as major constituents. By carbo thermal reduction in a plasma reactor under Ar atmosspere, SiO_2 is converted to SiC by the following reaction;

$$SiO_2 + 3C \rightarrow SiC + 2CO$$

For full conversion of SiO_2, an additional amount of carbon is added to the flyash before the chemical reaction occurs in the reactor. Addition of excess carbon is based on stoichiometric requirement of carbon, necessary for complete reduction of SiO_2 in the as received flyash. The comparison of diffraction pattern of the two materials confirms the conversion of SiO_2 to SiC [21]. Chemical analysis shows presence 2.8% carbon in the treated flyash, which corroborates to the findings of diffraction pattern.

SEM micrographs with EDS analysis of the plasma treated flyash powder is shown in Fig. 6a–c. The unique feature of the micrograph is that, there are whiskers of SiC, formed by the above reaction. These whiskers have high aspect ratio (40–50). The EDS analysis confirms presence of elements such as Al, Si, and C in the region where whiskers are formed. The reasons for better tribological properties of the novel Al-6061-PSFA composite are as follows.

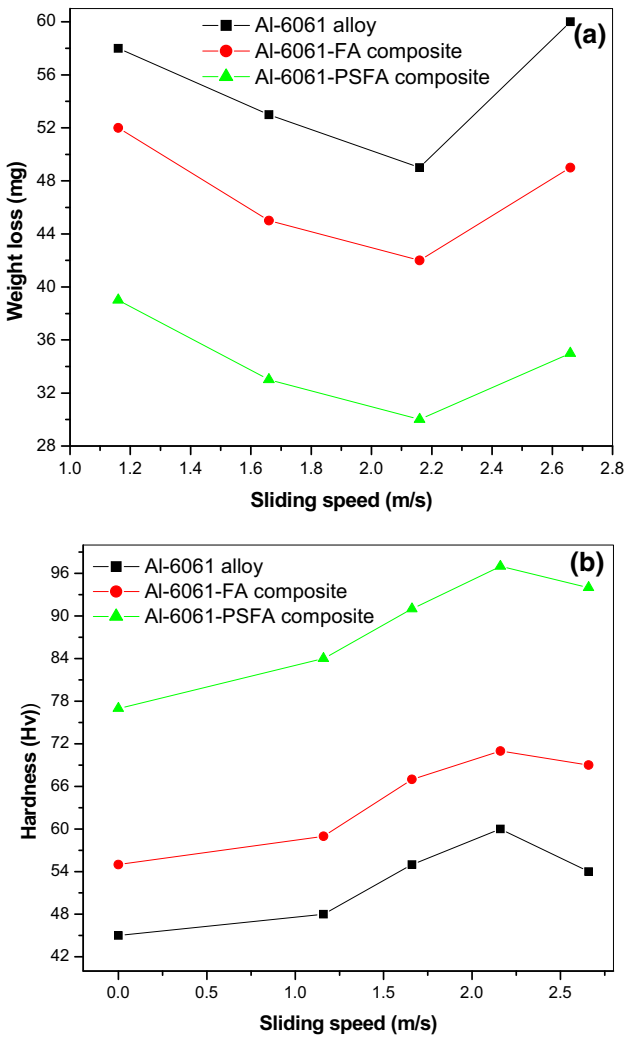

Fig. 7 Variation of **a** weight loss, and **b** hardness with sliding speed (Load: 40 N, sliding distance: 5000 m)

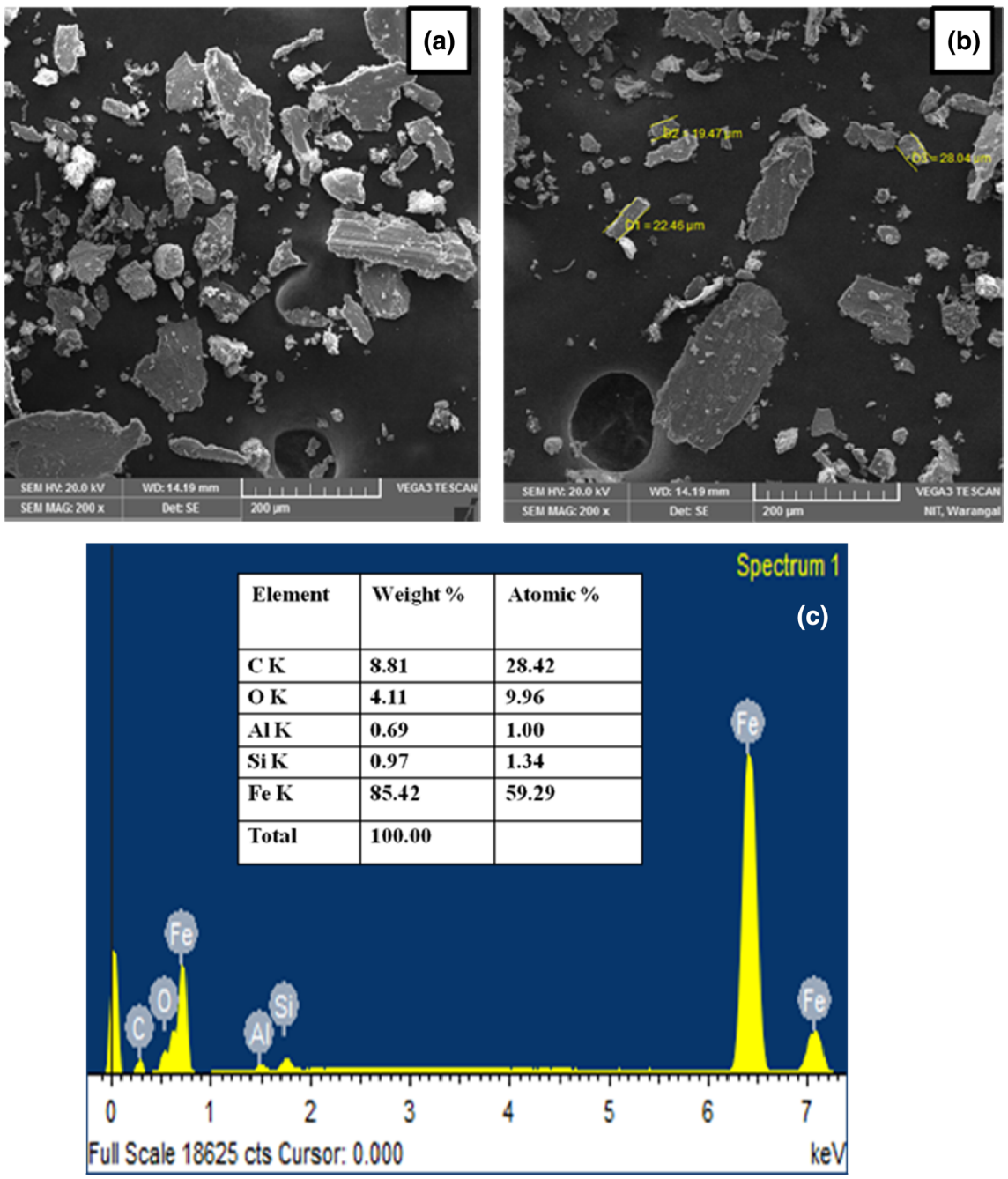

Fig. 8 **a**, **b** Representative SEM micrographs, and **c** EDS analyses of worn out debris of composite

a. The novel alloy composite (Al-6061-PSFA) is dispersed with SiC instead of SiO_2 as in other alloy composite (Al-6061-FA). Hardness of SiC is $\sim$2800 kg/mm^2 versus $\sim$600 kg/mm^2 for SiO_2. Therefore, harder particle in the alloy matrix increases the abrasion resistance of the developed alloy composite.
b. The additional carbon input to the composite has increased the abrasion resistance of the material to a limited extent. Carbon as graphite acts as lubricant and reduces the coefficient of friction. While the test material rotates against the hard steel disc, small graphite particles form a film on the test sample, which is believed to reduce frictional force. However, carbon addition is restricted to within 3%, since excess carbon addition in the alloy composite will increase porosity of the alloy matrix, which in turn will reduce mechanical properties.
c. The in situ conversion of SiO_2 to SiC in the vicinity of Al_2O_3 in the flyash with whiskers morphology not only

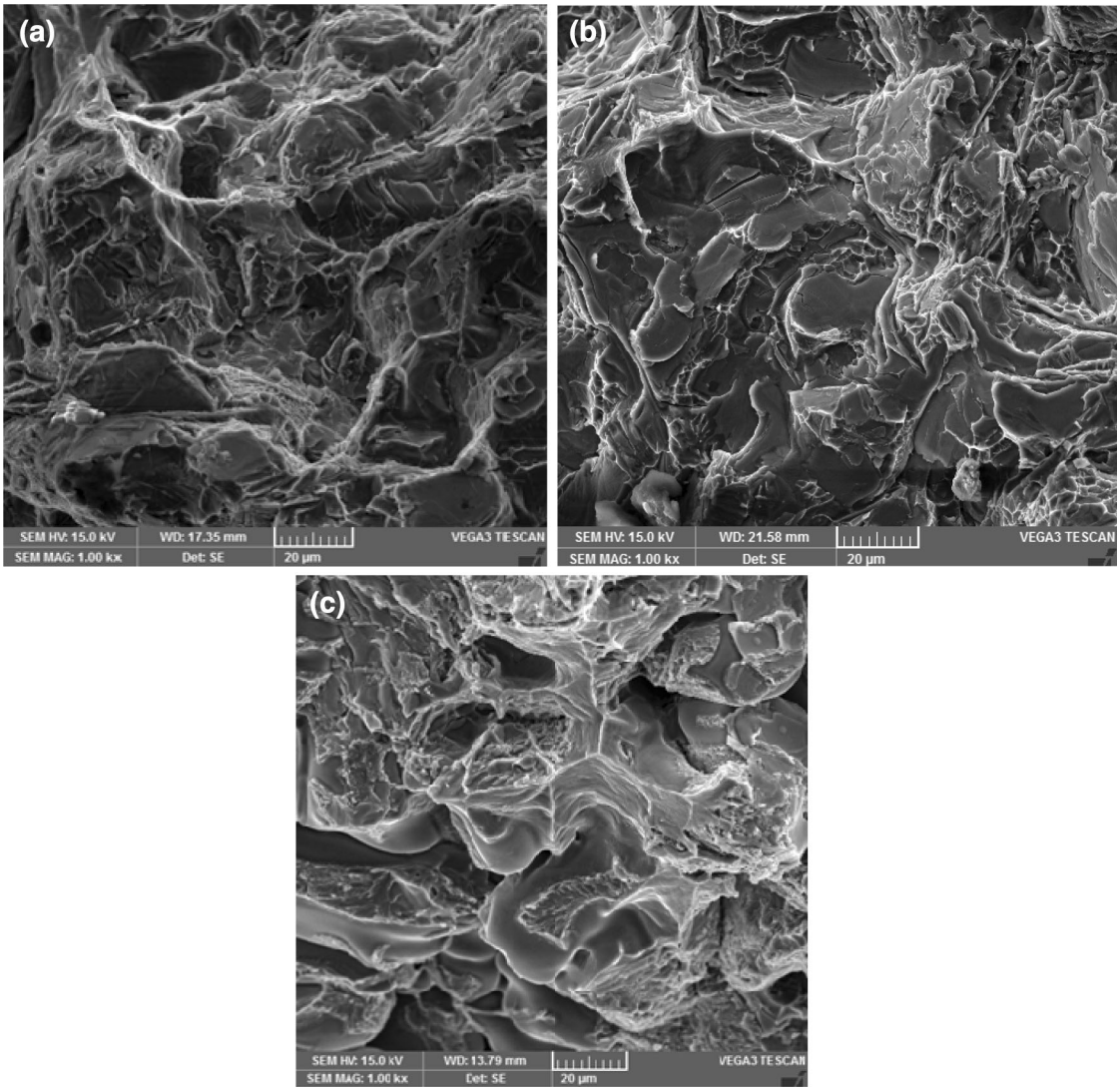

Fig. 9 SEM micrographs of fractured surface of; **a** Al-6061 alloy **b** Al-6061-FA composite, and **c** Al-6061-PSFA composite

helps to enhance the strength properties but also contributes to the tribological properties.

While discussing the mechanism of abrasion, one needs to appreciate that the process of abrasion is far more complicated than is expected, especially in case of composite materials. Based on the literature survey [22–25], the following discussion is initiated to understand the process of abrasion occurring in the present case. While the abrasion process is on, matrix starts abrading first. However, part of the energy input is spent for the plastic deformation. Extent of plastic deformation in the alloy matrix depends on the volume fraction of reinforcement particles. The lesser is the volume fraction of reinforcement particles occupied in the alloy matrix, the higher is the exposed surface of the matrix available for rubbing action. This will result in more plastic deformation in the matrix. Therefore, mechanism of abrasion will differ from case to case. In the present case, volume fraction is lower i.e. 10% as against 25% used by some researchers. Hence, the present analysis will differ from the findings of those who have used 25% volume fraction of reinforcement of alloy composite. Figure 7a, b show two plots i.e., weight loss and hardness plotted against sliding speed under identical condition, respectively. It is observed for both the cases that wear rate initially decreases and then increases beyond a critical value of speed. Similar trend is observed for hardness values also.

During initial stage of abrasion, mild wear occurs which is marked by smooth rubbed region. With the progress of rotation during the testing, the harder particles climb up to the surface and interact more with the rotating disc protecting the matrix from getting abraded and consequently abrasion rate decreases. This is described as oxidative wear where slow abrasion takes place [24]. Thus, combined

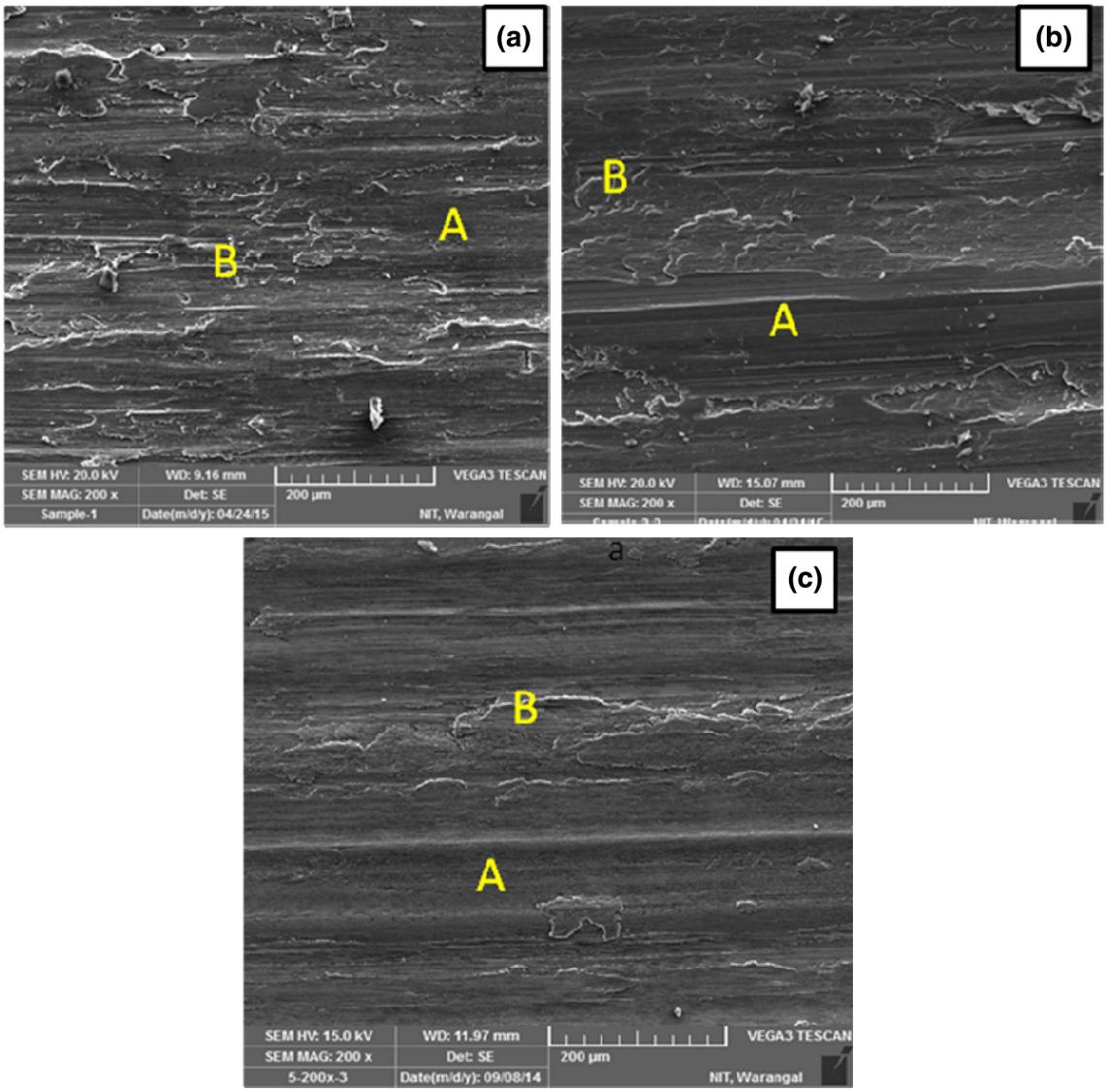

Fig. 10 SEM micrographss of worn out surface **a** Al-6061 alloy **b** Al-6061-FA composite, and **c** Al-6061-PSFA composite, (Load: 60 N, speed: 1.16 m/s, sliding distance: 5000 m)

effect of work hardening of the matrix and more exposure with harder particles of the test sample with the rotating disc causes decrease in wear rate (Fig. 7a).

By continuous rubbing action for a longer period, the harder particles appear frequently to rotating surface with higher applied load. Particles tend to crumble into fragments when stress reaches the fracture strength of the brittle constituents. There is accumulation of debris (Fig. 8a, b) on the pin surfaces during the wear run. As the depth of penetration in the ploughed region increases, delamination process begins and many particles are scooped out of the surface. As a result, there is continuous accumulation of debris. The temperature of the matrix increases simultaneously, which then reduces effect of work hardening by conventional process of recovery and recrystalization. Together, with the softening of the matrix, there are accumulation of harder ceramic particles from the test sample which helps in abrasion at a faster pace towards the end and above the critical speed (Fig. 6a). It is worth to mention here that hard steel disc gets abraded by continuous rubbing action of ceramic particles against the rotating disc. EDS analysis of debris has confirmed presence of Al, C, Si, Fe, and O (Fig. 8). In order to understand mechanism of abrasion, worn out surfaces are examined in SEM micrographs.

Figure 9a–c shows SEM micrographs of fractured surfaces of Al-6061 alloy, Al-6061-FA and Al-6061-PSFA composites, respectively. The appearances of fractured surfaces are similar in nature with some changes due to incorporation of reinforcement in the alloy. There are small

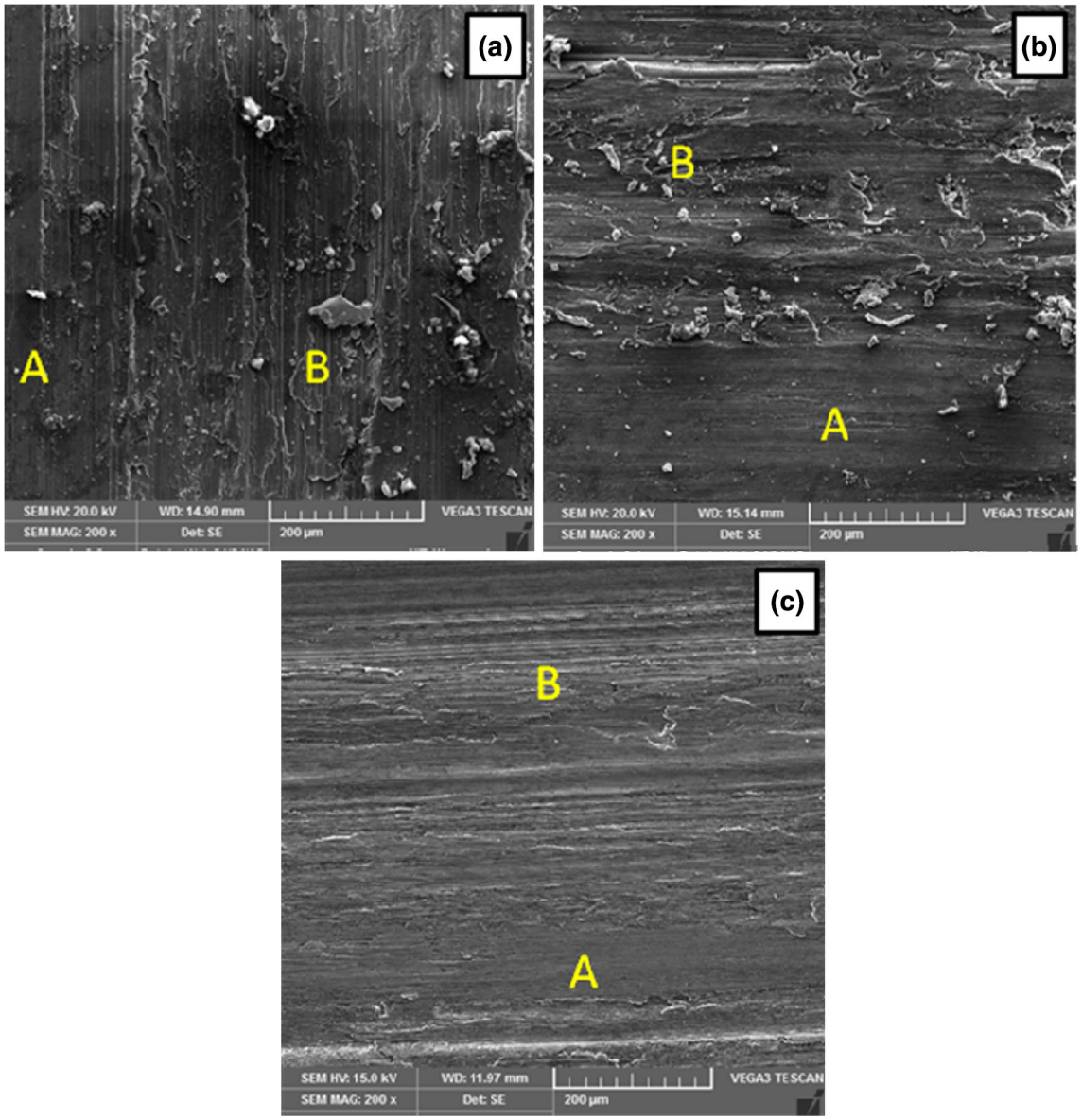

Fig. 11 SEM micrographs of worn out surface **a** Al-6061 alloy, **b** Al-6061-FA composite, **c** Al-6061-PSFA composite (Load: 40 N, speed: 2.16 m/s, sliding distance: 5000 m)

facets with dimples scattered widespread in the matrix in the as cast alloy. River pattern marking shows flow of cracks in the parallel plane formed by series of plateau and connecting planes. Figure 9b shows comparatively larger facets with some river pattern feature flowing along the boundary of larger facets containing hard particles. The presence of particle fracture and interfacial debonding are observed in Fig. 9b, c. Such localized damage occurs with the combined effect of internal and applied stresses. The coalescence of the localised damage at even higher strain levels lead to the final fracture of the composite material.

Figure 10a–c show SEM micrographs of worn out surfaces of three materials, tested under identical condition. These micrographs compare tribological behaviour of the three materials. Figures depict two distinct regions, marked 'A' and 'B'. Regions 'A' describes smooth ploughed region, (abrasive wear) which indicates lower wear rate, whereas region 'B' is deformed region (adhesive wear), indicating higher wear rate. The virgin alloy shows more adhesive wear in comparison to the other two composite materials. The least affected material is the developed novel Al-6061-PSFA composite.

Figure 11a–c show similar SEM micrographs for worn out surfaces, tested at lower load and sliding speed. General features of three micrographs are similar to those described in the previous paragraph. Detailed analyses of worn out surfaces of virgin alloy indicate patches of damaged region (adhesive wear), resulting from the crack

generation and propagation along the grooves. The surface, thus, features deep ridges with appreciable amount of damaged region in contrast to two other composites. The developed Al-6061-PSFA composite has shown the least rough region with shallow ridges. The above discussion has conclusively shown that use of developed alloy composite will be an interesting proposition for future applications.

4 Conclusions

1. A novel Al-6061 alloy based hybrid composite is developed indigenously suitable for industrial applications.
2. The weight loss of the virgin alloy is higher in absence of any hard dispersed particles, in contrast to the two other composites.
3. The enhancement of strength and tribological properties are attributed to the unique features of the microstructure developed by carbo-thermal treatment of flyash.
4. SiC in the form of whiskers have improved strength as well as specific strength.
5. The developed novel Al-6061 alloy based hybrid composite (Al-6061-PSFA) has enabled two fold higher wear resistance of the alloy based novel hybrid composite in comparison to the virgin alloy and 1.5 times higher to Al-6061-FA composite.
6. Decreasing weight loss with increasing sliding distance at initial stage is attributed to the combined effect of work hardening of the matrix and intensive interaction of hard oxide particles (oxidative wear) with the rotating steel disc.
7. Higher weight loss of the material above a critical speed is due to work softening of the matrix and rubbing of the test specimen against delaminated hard particles in the debris.
8. The virgin alloy shows adhesive nature of wear indicating high weight loss, whereas the developed Al-6061 alloy composites shows abrasive nature of wear which indicates lower weight loss of the material.

References

1. Rawal S, *JOM* **53** (2001) 14.
2. Miracle D B, *Compos Sci Technol* **65** (2005) 2526.
3. Logsdon W A, and Liaw P K, *Eng Fract Mech* **24** (1986) 737.
4. Rohatgi P K, Guo R Q, Huang P, and Ray S, *Metall Mater Trans A* **28** (1997) 245.
5. Prasad S V, and Asthana R, *Tribol Lett* **17** (2004) 445.
6. Rohatgi P K, Kim J K, Gupta N, Simon A, and Daoud A, *Compos Part A* **37** (2006) 430.
7. Suresh N, Venkateswaran S, Seetharamu S, *Mater Sci-Poland* **28** (2010) 55.
8. Mazahery A, *J Compos Mater* **45** (2011) 2579.
9. Guo RQ, Rohatgi PK, and Nath D, *J Mater Sci* **32** (1997) 3971.
10. Charles S, and Arunachalam V P, Indian *J Eng Mater Sci* **11** (2004) 473.
11. Rajan T P D, Pillai R M, and Pai B C, *J Mater Sci* **33** (1998) 3491.
12. Shanmughasundaram P, *Eur J Sci Res* **63** (2011) 204.
13. Milan M T, and Bowen P J, *Mater Eng Perform* **13** (2004) 775.
14. Cerit A A, Karamiş M B, Nair F, and Yildizli K *Tribol Ind* **30** (2008) 31.
15. Sahin Y, and M Acilar, *Compos Part A* **34** (2003) 709.
16. Rohatgi P K, Ray S, and Liu Y, *Int Mater Rev* **37** (1992) 129.
17. Ted Guo M L, and Tsao CYA, *Compos Sci Technol* **60** (2000) 65.
18. Anilkumar H C, Hebbar H S, and Ravishankar H S, *Int J Mech Mater Eng* **6** (2011) 41.
19. Sudarshan, and Surappa M K, *Wear* **265** (2008) 349.
20. Siva S B V, Sahoo K L, Ganguly R I, and Dash R R, J *Mater Eng Perform* **21** (2012) 1226.
21. Govindarao R, Ganguly R I, Dash R R, Rao P S P, Reddy G S, and Singh S K. *Trans Indian Inst Met.* **68** (2015) 951.
22. Slipenyuk A, Kuprin V, Milman Y, Goncharuk V, and Eckert J, *Acta Mater* **54** (2006) 157.
23. Christman T, Needleman A, and Suresh S, *Acta Mater* **37** (1989) 3029.
24. Rao R N, Das S, Mondal D P, Dixit G, and Devi SLT, *Tribol Int* **60** (2013) 77.
25. Wilson S, and Alpas A T, *Wear* **212** (1997) 41.